

# Transients in sheared granular matter

Brian Utter\* and R. P. Behringer

*Department of Physics and Center for Nonlinear and Complex Systems,*

*Box 90305, Duke University, Durham, NC 27708*

(Dated: February 8, 2020)

## Abstract

As dense granular materials are sheared, a shear band and an anisotropic force network form. The approach to steady state behavior depends on the history of the packing and the existing force and contact network. We present experiments on shearing of dense granular matter in a 2D Couette geometry in which we probe the history and evolution of shear bands by measuring particle trajectories and stresses during transients. We find that when shearing is stopped and restarted in the same direction, steady state behavior is immediately reached, in agreement with the typical assumption that the system is quasistatic. Although some relaxation of the force network is observed when shearing is stopped, quasistatic behavior is maintained because the contact network remains essentially unchanged. When the direction of shear is reversed, a transient occurs in which stresses initially decrease, changes in the force network reach further into the bulk, and particles far from the wheel become more mobile. This occurs because the force network is fragile to changes transverse to the force network established under previous shear; particles must rearrange before becoming jammed again, thereby providing resistance to shear in the reversed direction. The strong force network is reestablished after displacing the shearing surface  $\approx 3d$ , where  $d$  is the mean grain diameter. Steady state velocity profiles are reached after a shear of  $\leq 30d$ . Particles immediately outside of the shear band move on average less than 1 diameter before becoming jammed again. We also examine particle rotation during this transient and find that mean particle spin decreases during the transient, which is related to the fact that grains are not interlocked as strongly.

---

\*Electronic address: utter@phy.duke.edu

## I. INTRODUCTION

Striking features of dense, sheared granular materials include the formation of shear bands, which is related to Reynold's dilatancy, and the presence of directionally oriented networks of force chains. While the steady state behavior of dense granular shear flows in two and three dimensions has been the subject of numerous studies, much less is known about the approach to steady state and the effects of changes in imposed shear [1, 2].

It is known that forces in compact granular materials are carried preferentially along a network of force chains in which a minority of the grains carry a majority of the load[3]. Imposing shear establishes an oriented network with force chains aligned preferentially so as to resist the applied shear[3, 4]. The force network is also correlated with the network of particle contacts, or texture. Grains are typically confined along certain jammed directions and free to move along other more fragile directions [5]. Small changes in the contact network are often sufficient to induce substantial changes in the force network [6]. The anisotropy in the force network impacts the trajectories of individual particles during shearing [7] and creates a more mobile and less mobile directions based on shearing history.

When shear is applied to a uniform state, there must be a transient during which the steady state response is achieved. If the imposed shear direction is altered, there must be additional transients during which the force network, texture, and mean particle velocities adjust.

The formation of an oriented network from an initially homogeneous state can be understood by the following argument[6]. Small-angle shear through an angle  $\phi$  can be decomposed into three parts. Two of these are compression and dilation along axes oriented at  $45^\circ$  to the direction of shearing. The third is a rotation by  $\phi/2$ . Force chains form primarily along the compressional direction. In the case of continuous shear deformation, such as that achieved in a Couette apparatus, the heuristic description of the force network also follows from this argument. In this case, the force chains form in response to the initial shear at roughly  $45^\circ$  to the shear direction, with an orientation that tends to resist further shearing. However, under sufficiently strong shear, the network cannot resist the motion of the shearing surface; it fails as particles roll and slip. Still, on average, the orientation of the strong network remains.

In this paper, we present experimental results on transient behavior in a 2D Couette

shearing experiment. The grains are photoelastic disks which allow measurement of the forces at the grain scale, thus revealing the force chain structures. In these experiments, we study the transients after changing the imposed shear. We generate these transients in one of four ways: 1) by imposing shear on a homogeneous packing; 2) by stopping steady shear and observing the relaxation to a static packing; 3) by stopping steady shear, then restarting in the same direction; or 4) by reversing the direction of shear after steady state behavior is reached. This work provides a 2D analogue to the work by Losert *et al.*[1, 2].

If the system is stopped and shear is re-applied in the same direction, steady state behavior should more or less immediately be produced (assuming slow, quasistatic shearing). That is, aside from some small effect from aging of the force network, the texture should provide a memory of where the system was stopped. If the system is sheared in the opposite direction after establishing a particular texture, a transient should be observed, as the force network is re-established so as to once again resist shear, after which the particles are again close to a jammed state.

Although one expects force chains to be strong along their primary direction, they are fragile in the transverse direction[5, 8]. The experiments by Losert and Kwon [1], using particle tracking techniques, underscore these expectations through their studies of transients in a 3D Couette flow. In their experiments, restarting shear in the same direction quickly reproduced steady state behavior, while reversing the shear direction created a transient in which particles far from the shearing wheel moved faster than at steady state. They attributed this increased mobility to a softness of granular matter in the direction perpendicular to the principle force axis in agreement with the picture of jammed and fragile directions. Although this interpretation is quite reasonable, the experiments by Losert and Kwon could not directly observe changes in the force network. The experiments described here provide imaging and quantitative data for the forces at the grain scale.

## II. EXPERIMENTAL DETAILS

A schematic of the experimental setup is shown in Fig. 1 [9]. The granular material (B) is a bidisperse mixture of photoelastic disks (thickness 0.32 cm) lying flat on a 2D Plexiglas surface. There are approximately 40,000 grains in a ratio of three small (diameter  $d_S = 0.42$  cm) to one large ( $d_L = 0.50$  cm) that are contained by an inner shearing wheel (inner

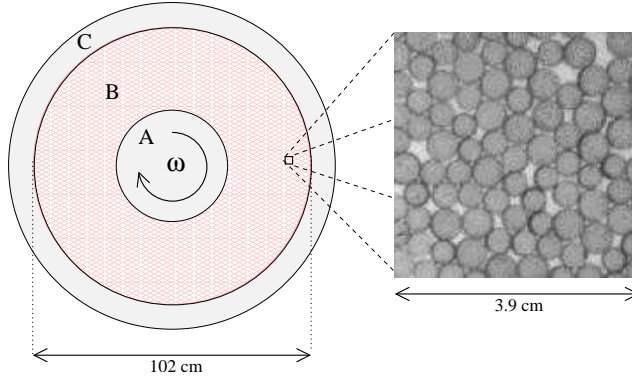


FIG. 1: Top view of the experimental apparatus. The shearing wheel (A) rotates at angular frequency  $\omega = 2\pi f$  shearing the granular material (B). The grains are contained by a stationary outer ring (C). On the right, an expanded view of the grains is shown.

radius,  $r_i \approx 20.5$  cm) (A) and a stationary outer ring (outer radius,  $r_o \approx 51$  cm) (C). The shearing wheel is rough at the particle scale and rotates at a frequency  $f$  of 0.1-10 mHz or a speed  $v \approx 0.013 - 1.3$  cm/s at the shearing surface. The mean packing fraction is  $\gamma \approx 0.76$  which can be changed between experiments by adjusting the number of particles. We image a subsection of the apparatus ( $\leq 10\%$ ) over long times (see images below). Each particle has a line across its diameter to easily measure its position, orientation, and size. Friction between the grains and the surface on which they lie is decreased by applying a fine powder and has been measured to be two orders of magnitude smaller than the force of a typical force chain [10].

Stresses are measured by a “gradient squared method” [10] in which the mean square gradient  $\langle G^2 \rangle$  of the image intensity is measured at each pixel and averaged. This technique is based on the properties of photoelasticity in which increased stress on a particle illuminated between crossed right and left circular polarizers leads to higher density of bright and dark bands and a larger spatial gradient in transmitted light intensity near a contact. We have previously established that  $\langle G^2 \rangle$  is proportional to the mean force on a particle for the range of forces appropriate to these experiments [6, 10].

The experiment is initially run for multiple revolutions of the shearing wheel to establish a steady state profile. The shearing is then abruptly stopped. The experiment can then be restarted in the same direction (same shear) or in the opposite direction (reverse shear). This procedure is repeated multiple times to observe average behavior, since fluctuations

dominate for individual runs, particularly in the force network. We present measurements of mean particle motion and stresses below.

### III. EXPERIMENTAL RESULTS

#### A. Overview and Organization of Results

Below, we describe several transient processes. The first of these is when shear is applied to a homogeneous packing. The second occurs when established steady-state shearing is stopped. We then consider what happens if shearing is stopped, allowed to relax for a modest length of time, and then restarted in the same direction. Finally, the main focus is determining what happens when steady-state shearing is stopped, and then shearing is restarted in the reverse direction.

#### B. Shearing a Homogeneous Packing

We first consider the case when the grains are initially uniformly distributed before shearing is applied. In Fig. 2, we show mean displacements of particles at different radial distances from the shearing surface. We bin data in the radial direction and plot mean displacement versus time for each bin. As expected, the disks are quickly pushed outwards to larger values of  $r$ . The tangential displacement also shows a fast response before particles become jammed and a slower steady state velocity is achieved. The shear band forms very quickly, within 5-10 s, corresponding to a displacement of under  $3d$  of the shearing surface. Once the shear band forms, the evolving force network is qualitatively similar to that seen at steady-state.

#### C. Relaxation

We now describe the relaxation after steady-state shearing is abruptly stopped. Although it may be expected that relaxation would not occur, that is not the case, as shown below. Other recent results have revealed a long time logarithmic relaxation of the force network [11].

Fig. 3 shows the measured stress as a function of time in three typical cases in which steady state shear was stopped at  $t = 0$ . In each case, we chose to stop the shearing wheel

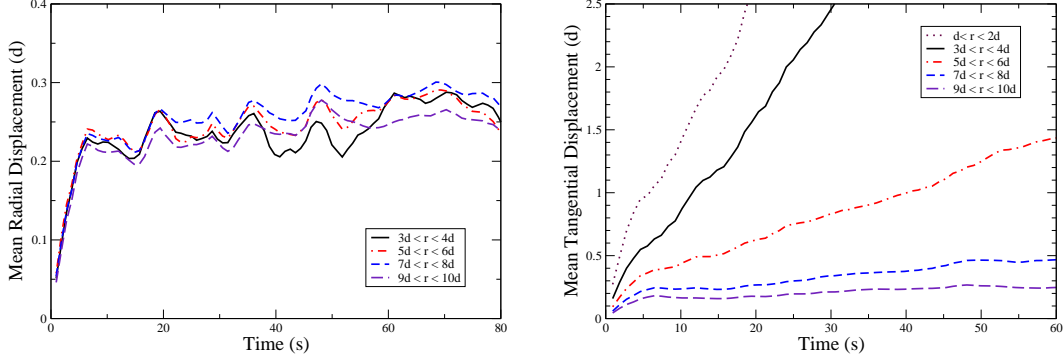


FIG. 2: Mean radial and tangential displacements during a transient starting from a uniform spatial distribution of particles ( $f = 1\text{mHz}$ ). After a transient of 5-10 s (shearing surface displacement = 3 d), a steady-state is

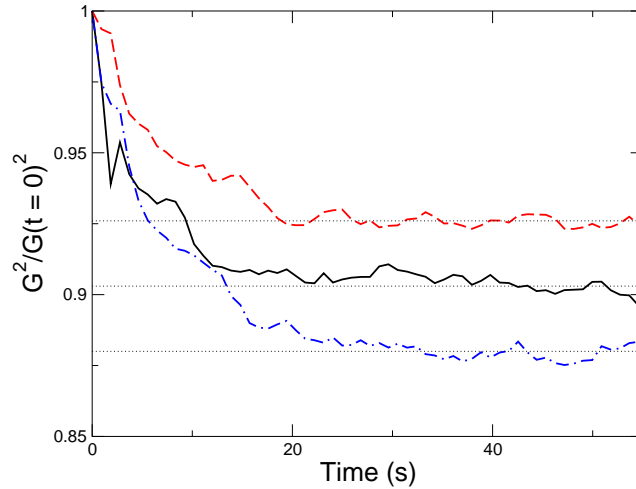


FIG. 3: Decay in mean stress vs. time. Stress is measured using a “gradient squared method” as described in the text. In three instances, we stopped the shearing ( $t = 0$ ) at a point of large stress within the field of view, and we then observed the relaxation of stress.

during a period of large stress. There was clearly a relaxation of stress over a few 10’s of seconds. During this time, the overall force network remained largely unchanged, although a few of the stronger force chains broke or relaxed. We show the network relaxation explicitly in Fig. 4. Here, the images correspond to when shear is stopped (4A), after 50 s (4B), and the difference between the first two images (4C). In Fig. 4C, white indicates an increase of force, and dark indicates a decrease of force. In addition, the bars on some of the particles close to the shearing surface shifted slightly. The relaxation was confined to the shear band

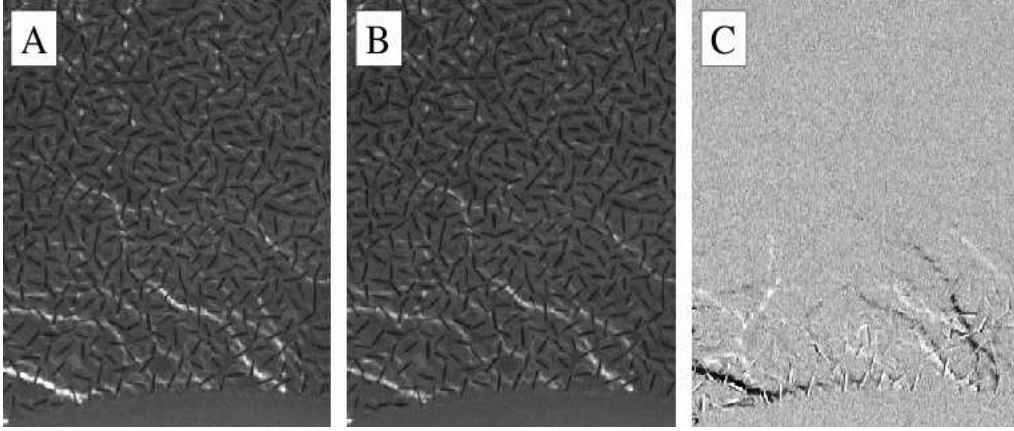


FIG. 4: Images shown (A) immediately after stopping steady shear to the left and (B) 50 seconds later. (C) The difference between the center and left images shows that particle motion is small and limited to grains close to the shearing wheel. Stronger stress chains have weakened (black) displacing the stress to other chains (white).

with small displacements observed in the grains within the first few layers of particles. Note that there was very little motion outside the first few layers and, even close to the shearing surface, measurable changes in the contact network were small.

#### D. Restarting Shear in the Same or Reverse Direction

When shearing is reversed, the anisotropic force network must readjust. Fig. 5 shows typical force chains during steady-state shearing along an initial direction (5A) and the force network with the shear reversed (5B). The white arrow represents the shear direction and the straight lines indicate the approximate orientation of the large stress chains. As described above, these form at approximately  $45^\circ$  to the direction of shear, so as to resist the shear force. The fragile directions are then at  $90^\circ$  to these lines [5, 8]. Note that upon reversing shear, the strong force direction switches to approximately align with the previous fragile direction. For comparison, Fig. 5C shows an image of the particles at the same magnification as that of the photoelastic force images.

We show velocity profiles immediately after restarting with the same or reverse shear in Fig. 6. The mean tangential velocity  $v_\theta$  is plotted versus distance from the shearing wheel in units of the mean particle scale  $d = (d_S + d_L)/2$ . Quantities are measured as functions

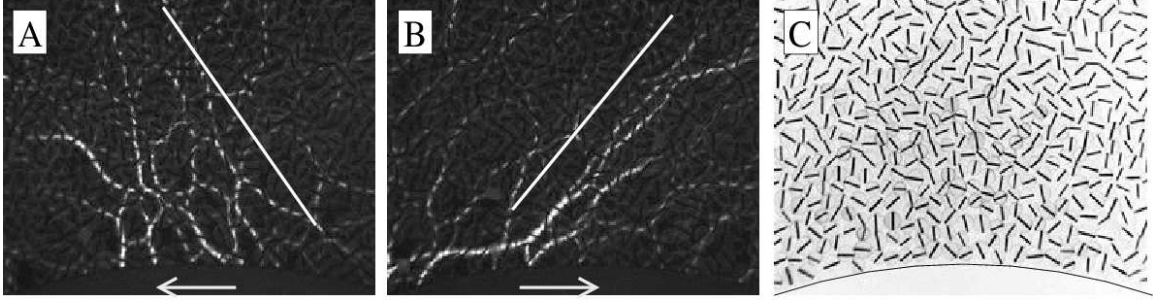


FIG. 5: Stress images during (A) same shear and (B) reverse shear. The arrow indicates the shearing direction and the solid lines indicate the approximate orientation of the strong stress network. (C) An image showing the grains at the same magnification.  $f = 1$  mHz.

of the radial distance  $r$  (where  $r = 0$  corresponds to the shearing surface) and averaged over azimuthal angle,  $\theta$ . Data is collected for the first 28 seconds after restarting shear, corresponding to a displacement of  $\approx 10d$  of the shearing surface. The curve for steady state behavior corresponds to a longer data run (1000 s), well after the initial transient has occurred. The velocity profile when restarting shear in the same direction is nearly indistinguishable from steady state behavior. This is expected for quasistatic flows. Although we observe some weak relaxation of the stress network (Fig. 3) substantial relaxation of the contact network does not occur. Hence, the initial velocity profiles and the profiles after restarting in the forward direction are virtually identical. That is, the force network experiences some aging once shearing is stopped [11], but there is essentially no change in the contact network, so the system can be regarded as quasi-static under shearing.

When shearing is initiated in the reverse direction, there is a transient in the velocity profile. Grains outside of the original shear band become unjammed and, consequently, move more because they are now being pushed along the fragile direction. The effect is not as strong right next to the shearing surface. These grains are initially pushed away from the shearing surface because there is initially no strong force network to resist this type of motion. Fig. 6B shows an expanded view of Fig. 6A. There, it is clear that particles which were previously jammed ( $7d < r < 12.5d$ ) are now mobile.

We also examine where significant changes in the force network occur, following the procedure used in Fig. 4C. In Fig. 7, we show difference images between the state immediately after steady-state shearing was stopped and the state 28 s after restarting shear ( $10d$  displacement of shearing surface). These images contrast the two cases of shearing in the same

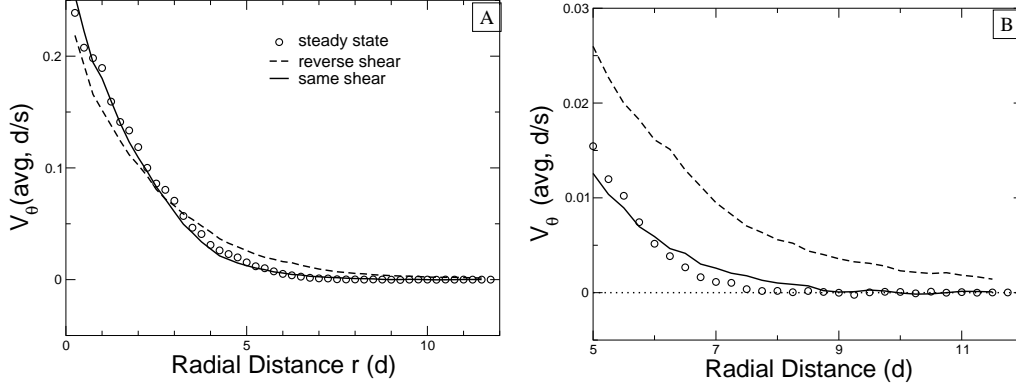


FIG. 6: Mean tangential velocity vs. radial distance from the shearing wheel for six runs ( $f = 1\text{mHz}$ ). Continuing the same shear direction (solid line) is indistinguishable from the steady state profile ( $\circ$ ) while reversing shear (dashed line) is clearly different. The figure on the right is an expanded view of that on the left. Particles that were jammed at steady state (far from shearing wheel) are now mobile, i.e. granular matter is fragile when forces are applied in a direction that is normal to the established texture. Here, the shearing rate is  $f = 1\text{ mHz}$ . These data were obtained in both cases during the first 28 seconds after (re)imposing shear.

and reverse directions. For each run, we use the magnitude of the difference image (i.e. deviation from grey, where grey indicates regions where no change has occurred) such that chains that form or disappear in the intervening time both contribute equally to the resulting intensity. In both difference images, we show the average from 6 runs and adjust the contrast to highlight the changes at the edge of the shear band. We also show a scale bar of length  $10d$ . In each case, significant changes in the force network are predominantly confined to the shear band ( $r < 10d$ ) as expected. However, upon reversing shear, changes in the force network reach further into the bulk, including the region where particles are initially more mobile ( $8 - 12d$ ). In Fig. 7C, we plot the (unadjusted) mean intensity versus radial distance from the shearing surface for the data used to construct Fig. 7A and B. There it is evident that changes in the force network reach further into the bulk when shear is reversed.

We now ask how long the increased mobility state lasts, and how far particles move before becoming jammed again. In Fig. 8, we show the mean displacement versus time, averaged over four runs, for particles at different distances from the shearing surface when the shearing direction is reversed. After an initial transient ( $t \lesssim 60\text{ s}$ ), trajectories follow  $r\Delta\theta = v_{avg}\Delta t$ . The straight lines are fits to the displacement versus time data after the transient (100-325

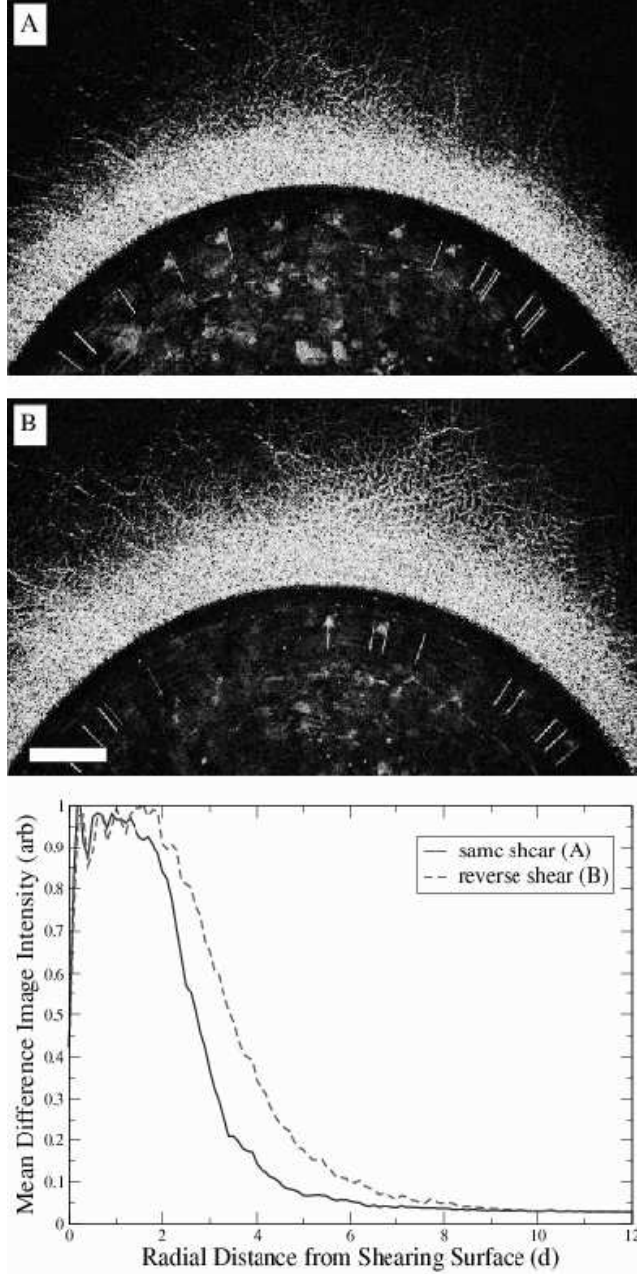


FIG. 7: Difference images showing magnitude of changes in force network during transients for (A) same shear and (B) reverse shear. Each image is an average of six runs. The contrast has been enhanced to emphasize the differences at the edge of the shear band. In (C) we show the mean intensity of the original images versus radial distance from the shearing surface.

s). The short line segments at the end of each curve indicate the expected slope  $v_{avg}$  based on the steady state velocity profile in Fig. 6. Particles that were previously jammed or moving slowly initially move relatively fast before reaching steady state conditions. This additional

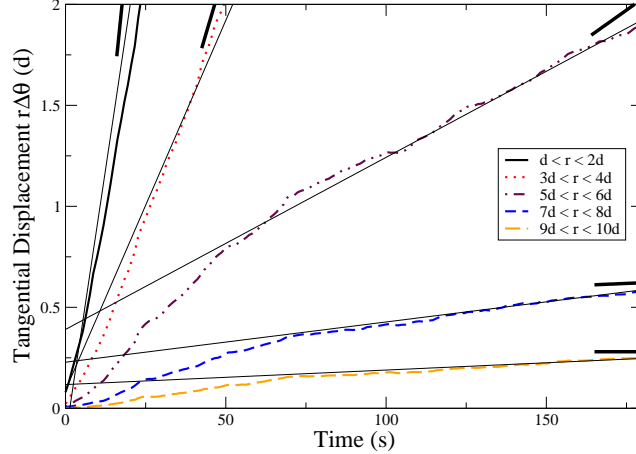


FIG. 8: Mean displacement versus time for particles at different radial distance after reversing shear. The data is for an average of four runs. Particles far from the shearing wheel ( $r \geq 7d$ ) move a fraction of a particle diameter  $d$  before reaching steady state velocity or becoming jammed again. The short line segments indicate the steady state slope expected from Fig. 6. Here, the shearing rate was  $f = 1$  mHz.

displacement due to the increased mobility during the transient ( $y$  intercept of straight line fits) is small, with displacements of less than  $1d$  needed to become jammed again. The existence of the additional displacement is qualitatively the same as that found by Losert *et al.*[1, 2], but the additional displacements are significantly smaller in our experiment. The timescale for readjustment is 50-100 seconds, corresponding to a displacement of the shearing wheel of 15-30  $d$ . Note that the transient is significantly longer than when applying shear to a homogeneous packing (Fig. 2). In agreement with Fig. 6, particles close to the wheel, initially move slower after shear reversal than at steady state, although the lag in displacement is small compared to the fluctuations in a steady state.

In Fig. 9, we have taken the data in Fig. 8 and removed the long time behavior (straight lines). Thus, the data in Fig. 9 eventually fluctuate around 0 and represent deviations from the mean steady state over time. At early times, negative values of the displacement show where particles have lagged and positive values show where they have advanced further than expected based on extrapolating back from the long-term steady state. After the 50-100 s transient, not only are steady state velocities reached, but also the mean motion of particles at different distances from the shearing is coordinated and grains at different  $r$  advance or lag in unison.

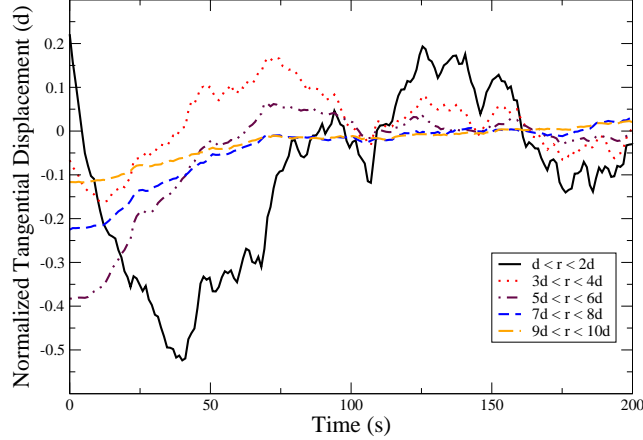


FIG. 9: Mean tangential displacement with the steady state fits (straight lines in Fig. 8) subtracted off. At long times, the curves fluctuate around zero.

We also measure the mean stress during these transients using the  $\langle G^2 \rangle$  technique described above. Fig. 10 shows the mean stress integrated over all particles in  $r < 10d$ , for an average of six runs. There it is clear that for  $t < 7s$  there is no observable stress for the case where the shear direction has been reversed. Although the fluctuations are different for each run, the initial quiescent period is observed in each case and for multiple packing fraction ( $\gamma = 0.755, 0.76, 0.765$ ). This is similar to the 3D results of Toiya *et al.*[2], despite the fact that in 3D, there is a compaction of the system [1]. Note that the stress readjusts on a smaller time scale than that for velocity relaxation. Qualitatively, the force network appears similar to the steady-state network after  $t \simeq 10s$ . Additional small adjustments of the force network might occur during the velocity relaxation, but they are not evident due to the strong fluctuations.

We study particle rotations during the transients in Fig. 11, where we show the mean particle rotation rate versus distance from the shearing wheel. The negative peak close to the shearing wheel reflects particles in contact with the wheel which are counter-rotating (Fig. 11A). If all particles in the innermost layer were stationary and counter-rotating with the shearing wheel, the mean rotation rate or spin,  $S$ , would be  $\approx -0.6$  rad/s, or in the scaled form  $S2\pi fr_i/d = -1$ . The positive peak for  $r \approx 1$  is due to the counter-rotation of the second layer (Fig. 11A). Further into the bulk ( $r > d$ ), the mean rotation is clockwise, which might be expected for frictional particles in a shear flow (Fig. 11B). That is, for the intermittent motion of a grain in the bulk, it is most likely that the neighbor further from

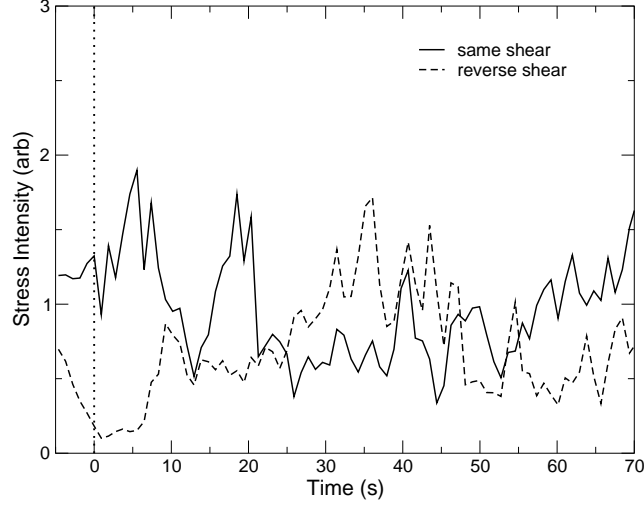


FIG. 10: Mean stress vs. time. There is initially no measurable stress upon reversing shear ( $t < 7s$ ).

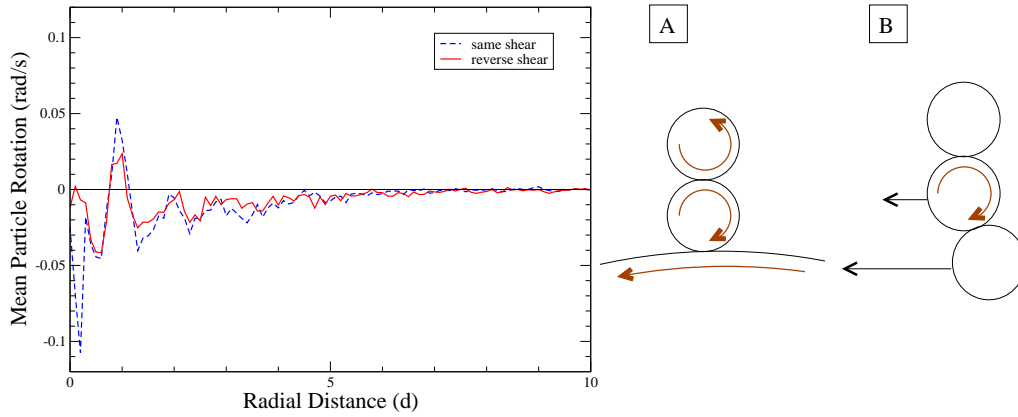


FIG. 11: Mean particle rotation versus radial distance. The mean behavior is influenced by (A) particles counter-rotating close to the shearing wheel and (B) particles rotating clockwise due to shear ( $r > 1$ ).

the shearing surface is nearly stationary while the neighbor closer to the shearing surface moves to the left, leading to clockwise rotation of the grain. The data is qualitatively similar when restarting shear in the same or reverse directions, but the magnitudes of the peaks is somewhat smaller during reverse shear since they are not interlocked as strongly. These results are similar to what was observed by Veje et al.[4].

## IV. CONCLUSIONS

We have studied the behavior of transients in a 2D granular Couette shear experiment. We find that when we restart shear in the same direction as previous steady state shearing, no significant transients occur. Even though some slow relaxation of the force network occurs, there is no transient because there are no significant changes in grain positions when shearing is stopped. In this sense, the process is quasistatic. When we reverse the shearing direction, transients do occur as the force network reforms. During this process, grains outside of the shear band are more mobile since they are pushed along an initially fragile direction. Photoelastic stress images support this picture. Mean grain displacements of less than a particle diameter are sufficient for particles far from the shearing surface to become jammed again and reach a nearly steady-state stress structure. Immediately after reversal, there is no measurable stress, since there is no pre-existing force network to resist shearing. During the transient however, changes in the force network for reverse shear reach further into the bulk as compared to what occurs for restarting shear in the same direction. The strong force network is reestablished after displacing the shearing surface by  $\sim 3d$ . Steady state velocity profiles are reached after a displacement of  $\leq 30d$ . Reversing the shear decreases the magnitudes of the particle spins slightly since grains are not interlocked as strongly, but the spin profile still maintains the same qualitative shape, with an overall reversal of sign.

**Acknowledgement** We appreciate a number of helpful discussions with Prof. Wolfgang Losert. This work has been supported by the National Science Foundation through grants DMR-0137119, DMS-0204677 and DMS-0244492, and by NASA grant NAG3-2372.

- 
- [1] W. Losert and G. Kwon, *Advances in Complex Systems* **4**, 369 (2001).
  - [2] M. Toiya, J. Stambaugh, and W. Losert, unpublished (2003).
  - [3] D. Howell, R. Behringer, and C. Veje, *Chaos* **9**, 559 (1999).
  - [4] C. Veje, D. Howell, and R. Behringer, *Physical Review E* **59**, 739 (1999).
  - [5] M. Cates, J. Wittmer, J.-P. Bouchaud, and P. Claudin, *Physical Review Letters* **81**, 1841 (1998).
  - [6] J. Geng, G. Reydellet, E. Clement, and R. P. Behringer, *cond-mat/0211031* (2003).
  - [7] B. Utter and R. P. Behringer, accepted to *Phys. Rev. E*,

<http://arxiv.org/abs/cond-mat/0309040> (2004).

- [8] F. Radjai, D. Wolf, M. Jean, and J.-j. Moreau, *Physical Review Letters* **80**, 61 (1998).
- [9] For details on a previous version of the experiment, see [3].
- [10] D. Howell, R. Behringer, and C. Veje, *Physical Review Letters* **82**, 5241 (1999).
- [11] R. R. Hartley and R. P. Behringer, *Nature* **421**, 928 (2003).